Available online at BCREC website: https://bcrec.id

Bulletin of Chemical Reaction Engineering & Catalysis, 17 (2) 2022, 250-262

Research Article

Sodium Silicate Catalyst for Synthesis Monoacylglycerol and Diacylglycerol-Rich Structured Lipids: Product Characteristic and Glycerolysis–Interesterification Kinetics

Inasanti Pandan Wangi[1], Supriyanto Supriyanto[1], Hary Sulistyo[2], Chusnul Hidayat[1,*]

[1]Department of Food and Agricultural Product Technology, Faculty of Agricultural Technology, Universitas Gadjah Mada, Jl. Flora No 1 Bulaksumur, Yogyakarta, Indonesia.
[2]Department of Chemical Engineering, Faculty of Engineering, Universitas Gadjah Mada, Jl. Grafika No 2 Yogyakarta, Indonesia.

Received: 30th December 2021; Revised: 22nd February 2022; Accepted: 23rd February 2022
Available online: 2nd March 2022; Published regularly: June 2022

Abstract

Sodium silicate as heterogeneous base catalysts is more environmentally friendly and easily separated by filtration. The objective of this research was to evaluate the activated sodium silicate as catalyst for synthesis of monoacylglycerol (MAG) and diacylglycerol (DAG)-rich structured lipids (SLs) from a palm olein-stearin blend. Sodium silicate was activated and functional group was characterized. Reaction was performed using 5% catalyst (w/w) at various reaction temperature (70–120 °C) for 3 h in a batch stirred tank reactor. Physical properties of SLs, such as melting point, slip melting point, and hardness of SLs were determined. Reaction kinetics were also evaluated. The results show that Si–O bending was reduced and shifted to a Si–O–Na and Si–O–Si functional groups after sodium silicate activation. Temperature had a significant effect on SLs composition at higher than 90 °C. An increase in temperature produced more MAG, resulting in better product physical properties. The best reaction condition was at 110 °C. Rate constants and the Arrhenius equation were also obtained for each reaction step. In summary, the activated sodium silicate catalyzed glycerolysis-interesterification reaction, which produced MAG and DAG at temperature higher than 90 °C. Therefore, the physical properties of SLs were improved.

Keywords: Glycerolysis-Interesterification; Structured Lipids; Monoacylglycerol and Diacylglycerol; Heterogeneous Base Catalyst; Reaction Kinetics

How to Cite: I.P. Wangi, S. Supriyanto, H. Sulistyo, C. Hidayat (2022). Sodium Silicate Catalyst for Synthesis Monoacylglycerol and Diacylglycerol-Rich Structured Lipids: Product Characteristic and Glycerolysis–Interesterification Kinetics. *Bulletin of Chemical Reaction Engineering & Catalysis*, 17(2), 250-262 (doi: 10.9767/bcrec.17.2.13306.250-262)

Permalink/DOI: https://doi.org/10.9767/bcrec.17.2.13306.250-262

1. Introduction

Structured lipids (SLs) are fats that have been chemically or enzymatically modified from their natural form to meet food and nutritional needs. The scope of SLs includes the manufacture of triacylglycerol (TAG), monoacylglycerol (MAG), diacylglycerol (DAG), and phospholipids [1]. MAG and DAG are emulsifiers that are widely applied to food products, which is as much as 75% of the total world use of emulsifiers and is also commonly used in bakery, margarine, dairy, and confectionery products because of their emulsifying, stabilizing, and conditioning properties [2,3]. MAG and DAG have high melting points so that they are solid at room temperature [4]. The nature of MAG and

* Corresponding Author.
Email: chusnulhi@ugm.ac.id (C. Hidayat);
Telp: +62-274-589797, Fax: +62-274-589797

DAG can be utilized as SLs to increase the melting point (MP) and hardness of the resulting product.

The synthesis of SLs containing MAG and DAG is usually carried out by glycerolysis, in which oil reacts with glycerol to produce MAG and DAG products [3]. However, glycerolysis is usually only performed by one type of fat/oil blend. Production of MAG and DAG-rich SLs from blended oil can be carried out by simultaneously combining the glycerolysis reaction with interesterification, called the glycerolysis-interesterification reaction [5,6]. Glycerolysis-interesterification is a simultaneous reaction between glycerolysis and interesterification. This combination can improve the physicochemical properties of the desired product [5,6].

Some importance kinetic studies on glycerolysis-interesterification are to understand the reaction mechanism, develop a mathematical model of the reaction rate, and evaluate the operating parameters of the system [7]. Reaction kinetic studies are generally carried out by Arrhenius equation, in which different operating conditions lead to various Arrhenius parameters [8–14]. Although the reaction kinetic studies of numerous types of fat and oil had been widely reported previously, the analysis of blended fat or oil has not been much reported yet [12–15]. Therefore, it will be an interesting subject to further study.

MAG and DAG synthesis can be carried out enzymatically or chemically. Chemical processes using heterogeneous base catalysts provide a more efficient and environmentally friendly approach. They were (i) easily separated by filtration, (ii) could avoid the formation of by-products, (iv) did not require a neutralization step to stop the reaction, and (v) could be reused for subsequent processes [16,17]. Several studies using heterogeneous base catalysts, such as MgO/Mg-Al hydrotalcite, hydrotalcite + K_2CO_3, and MgO supported - KOH catalyst, resulted in relatively high yields [16–18]. One of the heterogeneous base catalysts that can be used is the sodium silicate (Na-silicate) catalyst. Sodium silicate catalyst is a heterogeneous base catalyst. It has high catalytic activity and has characteristics that resemble a supported-solid base catalyst. This was shown from several studies that have been carried out on the manufacture of biodiesel using the catalyst [8,19,20]. To the best of our knowledge, the application of sodium silicate catalyst in SLs synthesis and/or glycerolysis process has limitedly been used. Therefore, this research was conducted using a sodium silicate base catalyst for the MAG and DAG-rich SLs synthesis through the glycerolysis-interesterification reaction.

The purpose of this research was to evaluate the reaction kinetics and acyl glycerol profile of the glycerolysis-interesterification process using activated sodium silicate. In this research, MAG and DAG-rich structured lipids were synthesized from a palm stearin-olein blend using activated sodium silicate as the heterogeneous base catalyst. The reactions were modeled, and their rate constants were determined based on the reaction model. The effect of temperature on rate constants was predicted using the Arrhenius equation. Furthermore, the physical properties, such as melting profile and hardness of the product, and the interaction between the sodium silicate catalyst and SLs products were also evaluated.

2. Materials and Methods

2.1 Materials

Refined Bleached and Deodorized Palm Stearin (RBDPS) (IV 38.56 I2 / 100 g fat) and Palm Olein were obtained from PT. Sinar Mas (Surabaya, Indonesia). Glycerol, NaOH, and silica gel were obtained from Merck KGaA (Darmstadt, Germany). A molecular sieve was obtained from Sigma-Aldrich (Missouri, USA).

2.2 Sodium Silicate Catalyst Activation

The sodium silicate was activated according to Perdana *et al.* [20]. Sodium hydroxide (NaOH) was weighed as much as 10 g, then dissolved in 10 mL of aquadest and stirred until homogeneous. The silica gel (7.5 g) was added gradually into the NaOH solution while stirring until a gel was formed. The gel was added to the porcelain crucible and heated in the furnace at 400 °C for 3 h. The activated gel was crushed with mortar. The result was sodium silicate powder, which could be directly used as a catalyst in the glycerolysis-interesterification reaction.

2.3 Glycerolysis-Interesterification Reaction at Various Temperature

The glycerolysis-interesterification reaction process was modified from Subroto *et al.* [5]. Palm stearin and palm olein ratio of 1:4 (w/w) were blended, then called oil. The oil was reacted with glycerol with a molar ratio of oil : glycerol = 1:2. Sodium silicate catalyst was added as much as 5% (w/w oil) and molecular sieve was added as much as 12% (w/w total reactant). The reaction was performed in a batch reactor at various temperatures (70, 80, 90,

100, 110, and 120 °C) and a stirring speed of 200 rpm for 3 h. Samples were taken at 0, 5, 10, 15, 30, 45, 60, 75, 90, 120, 150, and 180 min. The sample was then analyzed to determine TAG, MAG, and DAG concentrations. The properties of SLs products were also analyzed.

2.4 Characterization of Sodium Silicate Catalyst

Molecular structure and functional groups of sodium silicate catalyst were analyzed using Fourier Transfer Infrared (FTIR) Spectroscopy type 8201PC, Shimadzu Co., Japan, with a scanning range of 280–4000 cm^{-1}.

The total basicity of sodium silicate catalyst was analyzed using the Tanabe and Yamaguchi method [21,22]. About 20 mL of Benzene and 1 mL Bromthymol Blue indicator solution were added to a 100 mL Erlenmeyer flask. About 100 mg of 100–200 mesh sodium silicate catalyst was added to the solution. Sample was then titrated with 0.1 N Benzoic acid solutions until the green color disappeared.

2.5 Analysis of Acyl Glycerol Concentrations

The analysis of acyl glycerol was performed according to Subroto *et al.* [5]. The MAG, DAG, and TAG concentrations in each sample were analyzed using the Thin Layer Chromatography (TLC) scanner type Camag Automatic TLC Scanner III Dummy S/N (1.14.16) with Camag WinCATS software planar chromatography at wavelength 629 nm. Hexane, diethyl ether, and acetic acid (80:20:2, v/v/v) mixed solvent system was used as the mobile phase.

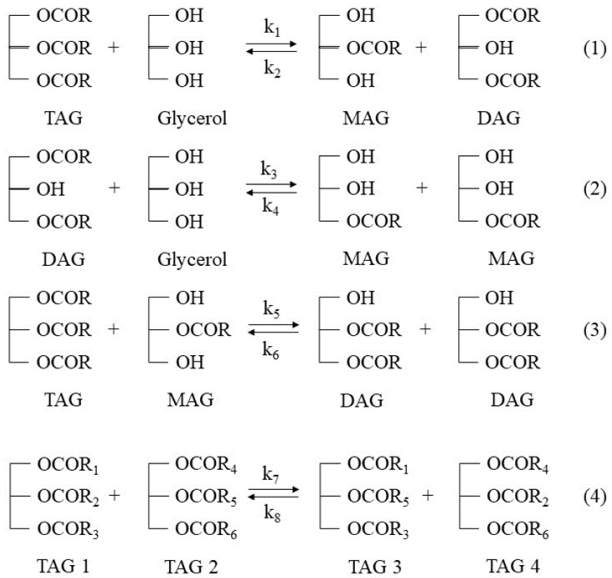

Figure 1. Schematic model of glycerolysis-interesterification reaction.

2.6 Reaction Kinetics Model

The glycerolysis-interesterification reaction was modeled as a combination of glycerolysis and interesterification reactions (Figure 1). In this reaction, TAG reacts with glycerol to produce MAG and DAG, namely the glycerolysis process. It can also react with another type of TAG with a different fatty acid profile, namely interesterification. This reaction can increase the possibility of the formation of desired fat because the obtained results are in the form of a mixture of MAG, DAG, and TAG SLs, which all play a role in shaping the physical, chemical, and functional properties of the targeted fat [5].

In this model, 4 possible reactions occur at the same time (Figure 1), in which reaction (1) to (3) represent the glycerolysis process and reaction (4) represents the interesterification. In the glycerolysis process, equation (1) is the initial reaction, then continued with Equation (2) which DAG byproduct reacts with the excess glycerol. If the MAG production is excess, the reaction will continue to Equation (3) which MAG reacts with the raw material to produce DAG. In the interesterification, the acyl migration only occurs between TAG.

The following assumptions were made in order to generate the reaction kinetics model: (a) Equation (1) expressed as the initial reaction can be considered as an irreversible reaction because of the excess of glycerol and low product concentration. Thus, the reversible reaction (represented as k_2) was neglected; (b) Since chemical catalyst leads to random glycerolysis-interesterification, the acyl migration on the glycerol backbone was challenging to identify because it varies widely over time. Thus, the acyl migration during the reaction was not analyzed, and the reaction kinetics determination was based on glycerolysis only; (c) A molecular sieve was used in this reaction. Thus, the forming of free fatty acid (FFA) during the reaction was neglected; (d) Catalyst was homogeneously dispersed in the system due to the mixing of reaction mixture at 200 rpm. Thus, mass transfer rate from the reactant to the catalyst can be neglected.

The following differential rate equations can then be used to describe the rate of change in concentration for each of the reaction components.

$$\frac{dC_{MAG}}{dt} = k_1 C_{TAG} C_{Gly} + 2k_3 C_{DAG} C_{Gly} - 2k_4 C_{MAG}^2 - k_5 C_{TAG} C_{MAG} + k_6 C_{DAG}^2 \quad (5)$$

$$\frac{dC_{DAG}}{dt} = k_1 C_{TAG} C_{Gly} - k_3 C_{DAG} C_{Gly} + k_4 C_{MAG}^2 + 2k_5 C_{TAG} C_{MAG} - 2k_6 C_{DAG}^2 \quad (6)$$

$$\frac{dC_{TAG}}{dt} = -k_1 C_{TAG} C_{Gly} - k_5 C_{TAG} C_{MAG} + k_6 C_{DAG}^2 \quad (7)$$

$$\frac{dC_{Gly}}{dt} = -k_1 C_{TAG} C_{Gly} - k_3 C_{DAG} C_{Gly} + k_4 C_{MAG}^2 \quad (8)$$

where, C is the concentration for each substance. *Gly* refers to glycerol. A computational code for the parameter estimation technique was written and implemented. The differential equations were solved with the *ode15s* subroutine, and the objective function was minimized with the *lsqnonlin* nonlinear data-fitting optimization subroutine.

The relationship between temperature and reaction rate constant was shown by the Arrhenius Equation (9).

$$k = A \exp\left(-\frac{Ea}{RT}\right) \quad (9)$$

where, k is the reaction rate constant, A is the exponential factor, Ea is the activation energy, R is the ideal gas constant, and T is the reaction temperature. From the Arrhenius Equation (9) it can be linearized as in Equation (10), so that the value of the activation energy (Ea) and the exponential factor (A) can be obtained.

$$\ln k = \ln A - \frac{Ea}{R}\frac{1}{T} \quad (10)$$

The obtained Arrhenius parameters were used to predict the MAG, DAG and TAG model at various temperature.

2.7 Analysis of Product Melting Point and Slip Melting Point

The slip melting point (SMP) analysis followed the AOCS Official Method Cc 3-25, and MP analysis followed the AOCS Official Method Cc 1-25 44, 45. Melted samples were inserted into a hematocrit tube about 1 cm height and then refrigerated overnight. Refrigerated samples were then heated gradually with the temperature increasing rate of about 0.5 °C/min until the samples flowed through the tube and changed into a clear liquid [23].

2.8 Analysis of Product Hardness

The product hardness was analyzed using the TA.XT Plus (Stable Micro Systems) type texture analyzer, with diameter probe 12.7 mm. Samples were prepared by melting the products at 80 °C for 15 min, then placed in a sample cup for about 1.5 cm in depth and continued by placing the samples at room temperature until hardened and then keeping the samples in a refrigerator (around 10 °C) for approximately 18 h. Before measurement, samples were taken out from the refrigerator and thawed for about 1 h. Measurements were performed at room temperature [5].

2.9 Statistical Analysis

A one-way analysis of variance (ANOVA) was used to analyze the data. Tukey's test was used to identify the difference between samples. P-value of <0.05 were considered significant.

3. Results and Discussion

3.1 Characteristics of Sodium Silicate Catalyst

The silica powder and the activated sodium silicate catalyst were analyzed using Fourier Transform Infra-Red (FTIR) spectroscopy to determine the functional structure applied on the catalyst surface. The result is shown in Figure 2. The dominant functional group in silica powder was silicate ion, represented as a downward peak at a wavelength value ~1100 cm^{-1} (Figure 2(A)). An absorption band of Si–O bending also occurred at ~470 cm^{-1} [19,24]. After the silica powder was reacted and activated into an activated sodium silicate catalyst, the intensity of the silicate ion and Si–O bending was reduced, shifted into a Si–O–Na and Si–O–Si functional groups, shown by a sharp downward peak at ~1000 cm^{-1} and ~890 cm^{-1}, respectively (Figure 2(B)).

These results prove that the activation process improved the structure of sodium silicate. The Na^+ ions were organized in various patterns around the non-bridging oxygen after activation [25]. Consequently, the ion exchange process becomes easier and can lead to a higher catalytic activity. Besides, the formation of the Si–O–Si group during the activation process shows that the SiO_4^{4-} tetrahedral shape changed from low polymerization conditions to high polymerization conditions. Changing the sodium silicate catalyst group to a more stable condition can provide a higher reaction conversion [19,25]. These transformations prove that the sodium silicate catalyst production and activation process was successful and can be used as a catalyst.

On the other hand, the total basicity of the activated sodium silicate catalyst was 9.19±0.08 mmol/g. This result was lower than the total basicity value reported by Guo *et al.* [19] at the same operating conditions. It is sug-

gested that the difference in basicity value is due to the difference in the source of silica gel. Although it has a slight difference, the basicity value of the activated sodium silicate catalyst was still higher than other heterogeneous base catalysts [21,22,26]. A higher basicity value may result in a higher conversion rate [19].

3.2 Conversion of Acyl Glycerol at Various Reaction Temperature

Glycerolysis-Interesterification was conducted in a batch stirred tank reactor at various temperatures using the activated sodium silicate catalyst. The conversions of TAG, MAG, and DAG at each variation are shown in

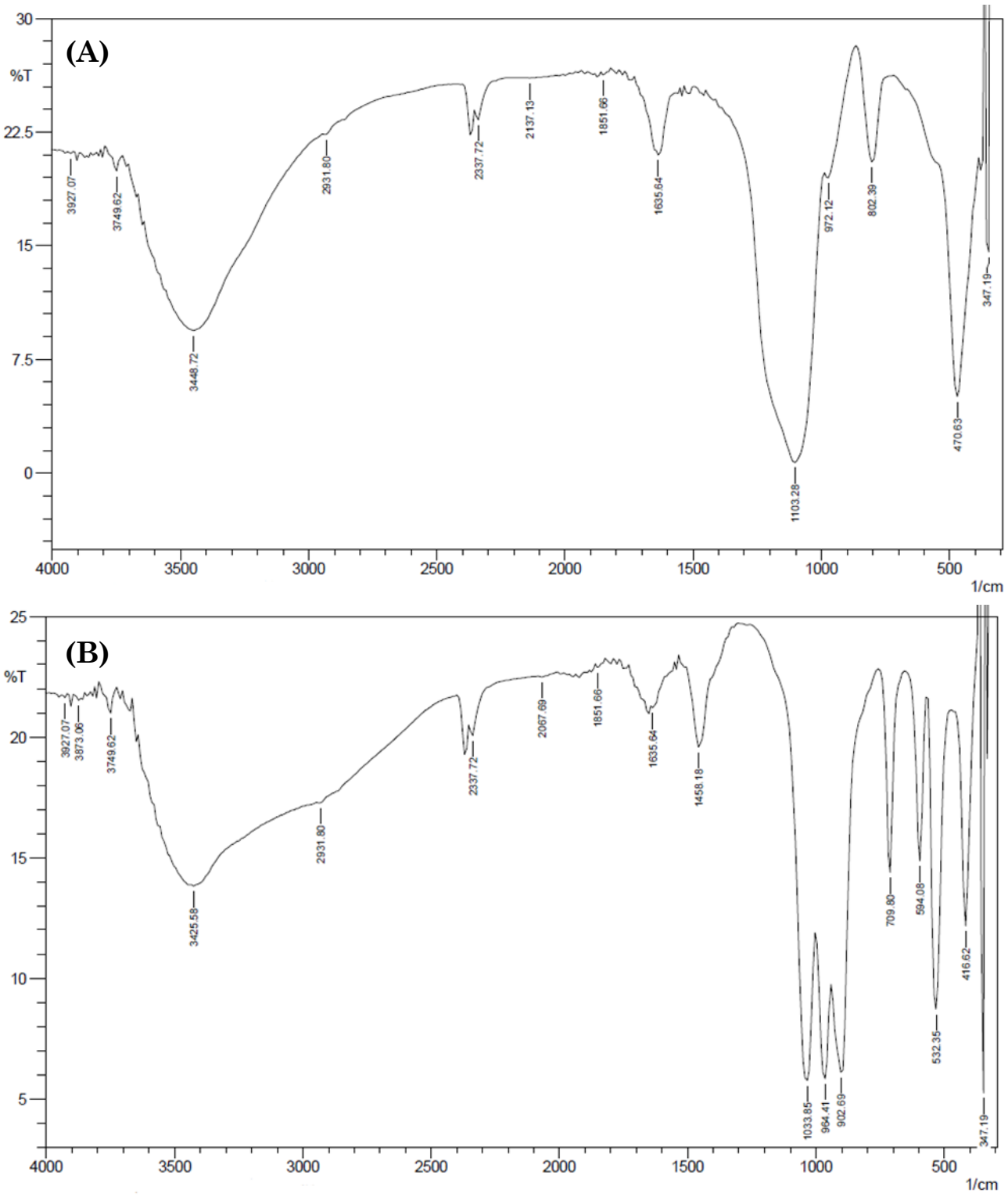

Figure 2. Functional structure of silica powder (A) and activated sodium silicate catalyst (B).

Figure 3. Most of them implied that the TAG concentration decreased while the concentrations of MAG and DAG increased with the increasing time. This result proves that the glycerolysis-interesterification reaction using the activated sodium silicate catalyst produce a combination of MAG, DAG, and TAG in the products.

MAG and DAG concentrations were lower than TAG concentration. It shows that not all TAGs were converted to MAG and DAG. Also, that TAG was still the dominant component in the product. At 90 °C and above, both the decrease in TAG and the increase in MAG and FFA were optimum. The high temperature helps catalysts extract hydrogen from glycerol

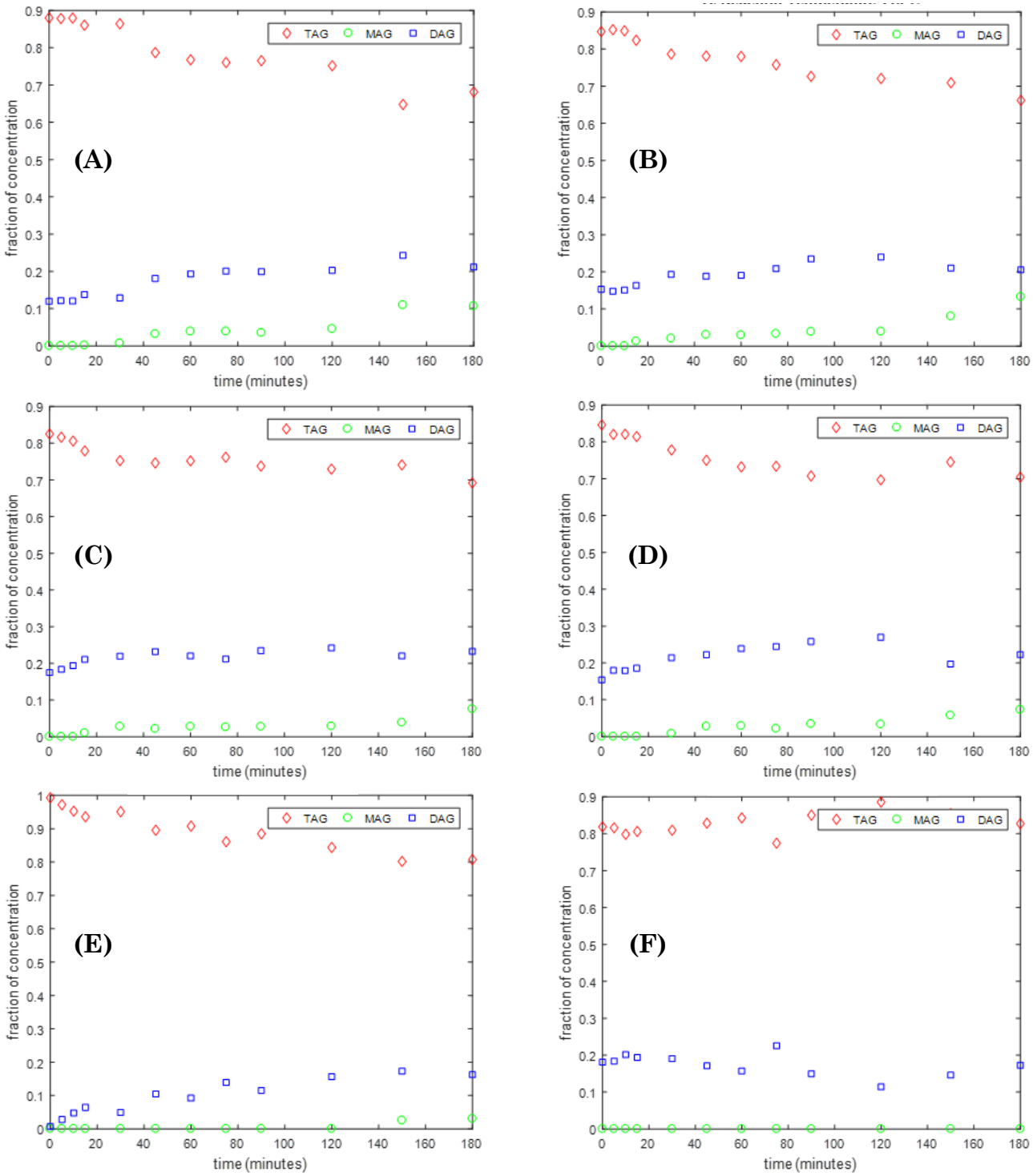

Figure 3. Conversion of TAG, MAG, and DAG at reaction temperature 120 °C (A), 110 °C (B), 100 °C (C), 90 °C (D), 80 °C (E) and 70 °C (F); stirring speed 200 rpm; and reaction time 3 h.

[28]. At 110 °C and 120 °C, the TAG, MAG, and DAG contents were at maximum value, which converted to 65%, 10%, and 25%, respectively. Temperature 110 °C was chosen to be the best-operating condition because it requires lower energy, although it has a similar result with 120°C.

It is suggested that the catalytic mechanism for glycerolysis-interesterification using the activated sodium silicate follows several steps [25,27]. The first step was the triglyceride enolate anion formation through alpha hydrogen abstraction by sodium silicate catalyst. The triglyceride enolate anion was then reacted with glycerol, leading to an ester interchange to form MAG and diglyceride anion. Finally, the proton was then transferred to diglyceride anion to form DAG in 2 possible ways: one is from the catalyst, and the other is from glycerol to produce more MAG. In addition, the triglyceride enolate anion was also able to react with MAG to produce DAG. This phenomenon may explain why the DAG value has a relatively stable value through time because it was always consumed and produced simultaneously during the reaction. The triglyceride enolate anion was also able to react with TAG as well to perform an interesterification mechanism. A beta-keto ester was formed during the process, which led to a TAG formation with a different fatty acid profile.

However, lower reaction temperature shows the opposite results. At the reaction temperature below 90 °C, the maximum reduction of TAG was around 80%, and the maximum rise of MAG was only about 3%. These results showed that low temperatures (especially 70°C and below) were insufficient to provide the appropriate MAG and DAG in products. Similar results were also reported by Zhong *et al.* [16] that 80°C was required and suitable to produce DAG by glycerolysis using KOH-MgO supported catalyst. Zhong *et al.* [16] also reported that CaO, MgO, and calcium hydroxide ($Ca(OH)_2$) catalysts were not effective for glycerolysis at a temperature lower than 100 °C.

3.3 Composition of TAG, MAG, and DAG in Structured Lipid Products

The composition of TAG, MAG, and DAG in the end products at each reaction temperature is presented in Table 1. It could be seen at high temperature, the TAG value were significantly different than the value at low temperature (Table 1). Lower TAG value shows that some of TAG were converted to MAG or DAG as products. These results proved that a higher reaction temperature could convert more TAG into products than a lower reaction temperature.

The MAG value differed significantly in every reaction temperature. The MAG content at 120 and 110 °C had the highest value, while 80 °C had the lowest value. These results also proved that a higher reaction temperature could produce more MAG than a lower reaction temperature. No MAG content was produced at 70 °C. It proved that this temperature was insufficient to initiate the glycerolysis-interesterification reaction. The reaction using low temperature had been previously reported by Subroto *et al.* [5]. The TAG content could be decreased up to 60%, MAG and DAG content increased up to 12% and 28%, respectively, using immobilized *C. antarctica* lipase as the catalyst at 50 °C for 24 h. Although it is possible to produce the SLs using low temperatures, a longer reaction time was needed. Thus, a higher temperature is still preferable in MAG and DAG-rich SLs production.

The DAG value for each reaction was not significantly different (Table 1). The value of DAG at the end of the reaction was also not much different from the initial value (Figure 3). This shows that there is only a small increase in the DAG value at the end product. In glycerolysis reaction, DAG is an intermediate product that will react with glycerol to produce MAG (Figure 1). However, the accumulation of MAG would react with the excess TAG to produce DAG, as the result, there is only a slight increase in the amount of DAG at the end of the reaction.

Table 1. Composition of TAG, MAG and DAG in structured lipid products.

Reaction Temperature (°C)	TAG (%)	MAG (%)	DAG (%)
120	$68.14 \pm 1.84^{a1)}$	10.68 ± 0.76^{ab}	21.18 ± 1.97^{a}
110	66.19 ± 3.15^{a}	13.26 ± 1.26^{a}	20.55 ± 1.89^{a}
100	71.03 ± 2.61^{a}	6.89 ± 0.95^{c}	22.09 ± 1.65^{a}
90	70.44 ± 5.54^{a}	7.30 ± 0.85^{bc}	22.26 ± 4.70^{a}
80	80.74 ± 0.46^{b}	3.03 ± 0.54^{d}	16.23 ± 0.08^{a}
70	82.72 ± 5.21^{b}	0.00 ± 0.00^{d}	17.28 ± 5.21^{a}

[1)] Different letters indicated significantly different values for each column ($p < 0.05$)

3.4 Physical Properties of Monoacylglycerol and Diacylglycerol-Rich Structured Lipids

The tested physical properties of the structured lipid products were SMP, MP, and product hardness. Results are shown in Table 2. Samples were compared with the previous data from Subroto *et al.* [5]. Compared to Palm Stearin-Palm Olein (PS-PO) blend, samples produced by glycerolysis-interesterification have significantly higher SMP and MP values (Table 2). SLs products had 1.34–1.46 times higher and 1.36–1.52 times higher SMP and MP than the PS-PO blend, respectively.

It can also be seen that samples produced in higher reaction temperatures have significantly different SMP and MP values. The previous discussion from Figure 2 implied that higher reaction temperature leads to more MAG and DAG production. MAG and DAG have a higher MP than TAG, ranging from 55.5 °C to 77.0 °C depending on the type of fatty acid. The presence of MAG and DAG will contribute to the increase and variety of the melting profile of the structured lipid products, while the PS-PO blend did not contain any MAG [4,5].

Product hardness value can also be seen in Table 2. PS-PO blend showed a drastically lower hardness value than the product with glycerolysis-interesterification at any reaction temperature, ranging from 4.65 to 15.90-fold increase. Some samples from higher reaction temperatures (with significantly higher MAG and DAG content) also had a relatively higher hardness value. This issue happens because MAG and DAG are solid at room temperature, so the presence of MAG and DAG will increase the hardness of the structured lipid products [4].

At temperature 120 °C, MP and hardness value were significantly lower than the value at 110°C. These results could happen because random interesterification between TAG from PS and TAG from PO also occurred in this system. Depending on the iodine value, PS contains TAG with the structure of palmitate-oleate-palmitate (p-o-p), palmitate-oleate-oleate (p-o-o) and palmitate-palmitate-palmitate (p-p-p) fatty acids around 27.5–46.5%, 12.9–31.5% and 14.3–37.4%, respectively. Whereas the TAG structure of PO consists of p-o-p, p-o-o and p-p-p around 28.7–40.9%, 24.5–43.7% and 2.4–3.9%, accordingly [29–31]. As mentioned earlier, the fatty acid type could affect the melting properties of the TAG, MAG, or DAG [4]. The random interesterification at 120 °C may produce a certain fatty acid profile that has lower MP properties. Thus, the melting profile and hardness can fluctuate for each reaction temperature.

3.5 Reaction Rate Constant and Arrhenius Parameters

At a reaction temperature of 70 °C (Table 1), MAG could not be formed under these oper-

Table 2. Physical properties of structured lipid products.

Reaction temperature (°C)	Slip Melting Point (°C)	Melting Point (°C)	Hardness (N)
120	55.95 ± 0.07[a1)]	59.90 ± 0.28[a]	23.89 ± 0.07[a]
110	54.50 ± 0.85[ab]	65.45 ± 0.64[b]	28.93 ± 0.08[b]
100	54.75 ± 0.35[ab]	67.10 ± 0.28[c]	14.31 ± 0.02[c]
90	51.75 ± 0.35[b]	65.15 ± 0.21[b]	12.35 ± 0.52[d]
80	51.30 ± 0.14[b]	63.10 ± 0.42[d]	14.27 ± 0.77[c]
70	53.90 ± 1.98[ab]	60.10 ± 0.42[a]	8.30 ± 0.53[e]
50[2)]	38.67 ± 0.29	44.67 ± 0.29	5.63 ± 0.59
PS-PO Blend[2)]	38.17 ± 0.29	44.00 ± 1.00	1.82 ± 0.31

[1)] Different letters indicated significantly different values for each column ($p < 0.05$)
[2)] Reference: Subroto *et al.* [5]

Table 3. Reaction rate constant and Arrhenius parameters.

Rate Constant	Reaction Temperature (°C)					Arrhenius Parameters	
	80	90	100	110	120	A	*Ea*/*R*
k_1	6.00×10^{-4}	8.00×10^{-4}	7.00×10^{-4}	8.00×10^{-4}	1.00×10^{-3}	6.66×10^{-2}	1676.2
k_3	9.00×10^{-4}	9.00×10^{-4}	6.00×10^{-4}	2.00×10^{-4}	0.00	9.82×10^{-12}	−6565.2
k_4	2.00×10^{-4}	0.00	0.00	0.00	0.00	n/a	n/a
k_5	1.26×10^{-2}	9.10×10^{-3}	5.20×10^{-3}	3.40×10^{-3}	1.70×10^{-3}	4.63×10^{-11}	−6897.2
k_6	2.10×10^{-3}	1.00×10^{-3}	4.00×10^{-4}	0.00	0.00	8.38×10^{-17}	−10904

ating conditions. We conclude that this temperature was not enough to initiate the glycerolysis-interesterification process. Thus, the calculation of rate constants was only based on the higher temperature data (80–120 °C) using Equations (5) to (8). As we assumed that the reversible reaction in equation (1) is neglected, the calculation of k_2 was also dismissed (Table 3).

The rate constants, k_1, k_3, and k_5 showed the product formation in Equations (1), (2), and (3). While rate constants k_4 and k_6 showed the reverse reaction (reactant formation) for Equations (2) and (3), respectively. From data obtained in Table 3, it could be seen that equation (2) was mainly irreversible, while Equation (3) was reversible only at a lower temperature. These results probably correlated to the usage of higher temperatures for the experimental procedure.

The high temperature helps to improve the mass transfer between oil and glycerol. Since oil and glycerol are viscous fluids at room temperature and they are immiscible, increasing the reaction temperature can drop the fluid's viscosity and improve the reaction between oil and glycerol [32]. Moreover, high temperature increases the kinetic energy between molecules, thus the intermolecular movement will increase and lead to a faster diffusion [33].

Glycerolysis also follows endothermic reaction and usually occurs at high temperatures [34–36]. According to Le Chatelier's principle, temperature affects the reaction equilibrium, which the higher the temperature, the more the reaction leads to the formation of products [37]. Thus, the reaction towards reactant formation will be minimal, and at some point, may lead to an irreversible reaction.

Since equation (1) was the initial reaction, it was assumed that this reaction was irreversible. Thus the calculation was only based on the product formation. The reaction constants for the reversible reaction in equations (2) and (3) were calculated. For those reactions, the reaction to generate products was more remarkable than product degradation to form the reactants. It is supported by the values of k_3 and k_5, which were greater than that of k_4 and k_6. Thus, all reactions contribute to the MAG and DAG product formation. The most influential reaction on the product formation was the Equation (3). It is proved by the highest reaction rate constant value (k_5) and the higher yield of DAG product than MAG at any reaction temperature. This issue is most likely happened due to the excess of TAG in the reactants and the accumulation of MAG over time, which shifts the reaction's equilibrium toward DAG formation, as reported by Moquin *et al.* [38].

The Arrhenius equation demonstrates the correlation between temperature and the reaction rate constant, as stated in equation (9). Since the value of k_4 (Table 3) was mostly zero for reaction at temperature 90 to 120 °C, it can be concluded that reaction (2) is irreversible. Thus the Arrhenius equation for k_4 was neglected. Therefore, the calculation of the Arrhenius constant and activation energy value was only based on k_1, k_3, k_5, and k_6 (Table 3).

From Table 3, it could be seen that the value of activation energy for k_3, k_5, and k_6 was negative, while k_1 was the only one that had a positive value. Since the activation energy value is less likely to be less than zero, it could be assumed that an intermediate complex could be formed during these reactions. Mozurkewich and Benson [39] explained that a tight transition state with low potential energy must be achieved to obtain a negative activation energy (Ea<0). This condition could be accomplished if the reaction undergoes a stable intermediate. The activation energy (Ea) is formed by the energy of transition state (E_{TS}) subtracted with the energy of reactant (E_R). At lower temperatures, the average energy of the transition state was lower than the average energy of the reactant, resulting in a negative value of activation energy. Nevertheless, in glycerolysis-interesterification, the activation energy for k_1 is the most important since it was the initial reaction.

3.6 Reaction Kinetics Model Evaluation

Figure 4 shows the experimental data of glycerolysis-interesterification compared to the kinetic model from the differential equation and Arrhenius parameters substitution. The difference between the experimental data and kinetic models for reaction temperature 120, 110, 100, 90, and 80 °C were 1.00×10^{-2}, 1.00×10^{-2}, 2.00×10^{-2}, 3.00×10^{-2}, and 3.00×10^{-2}, respectively. The difference of the kinetic model between the differential equation and Arrhenius parameters substitute were 4.00×10^{-8}, 9.00×10^{-8}, 4.00×10^{-8}, 6.00×10^{-7}, and 2.56×10^{-6}, respectively.

Kinetic models usually have a slight difference from the experimental data. Lionelli [40] explained that data are results of interactions between researchers and the world which are then processed as usable evidence to claim about a certain phenomenon, while models are conceptualized as representations of data. Data and models correspond to each other as they

are a representation of the real condition and proposed theory, respectively, with data being closer to real condition phenomena and models being closer to theory. Thus, connecting the theory and real conditions using the relation between experimental data and models would likely create a missing gap.

4. Conclusion

Activation of sodium silicate resulted in reduction of Si–O bending. It shifted to a Si–O–Na and Si–O–Si functional groups, which were shown by a sharp downward peak at ~1000 cm^{-1} and ~890 cm^{-1}, respectively. MAG content was not produced at 70 °C. However, the temperature has a significant effect on SLs at higher than 90 °C. The best condition for this reaction was at 110 °C. TAG, MAG, and DAG were up to 65%, 10%, and 25%, respectively at 110 °C and above. SLs products had SMP and MP 1.34–1.46 times and 1.36–1.52 times higher than the PS-PO blend, respectively. It showed a drastic increase in the hardness value than PS-PO blend ranging from 4.65 to 15.90-fold. Furthermore, MP and hardness value at 120 °C were significantly lower than the value at 110 °C. It is because of random interesterification between TAG of PS and TAG of PO in this system. Besides, kinetic

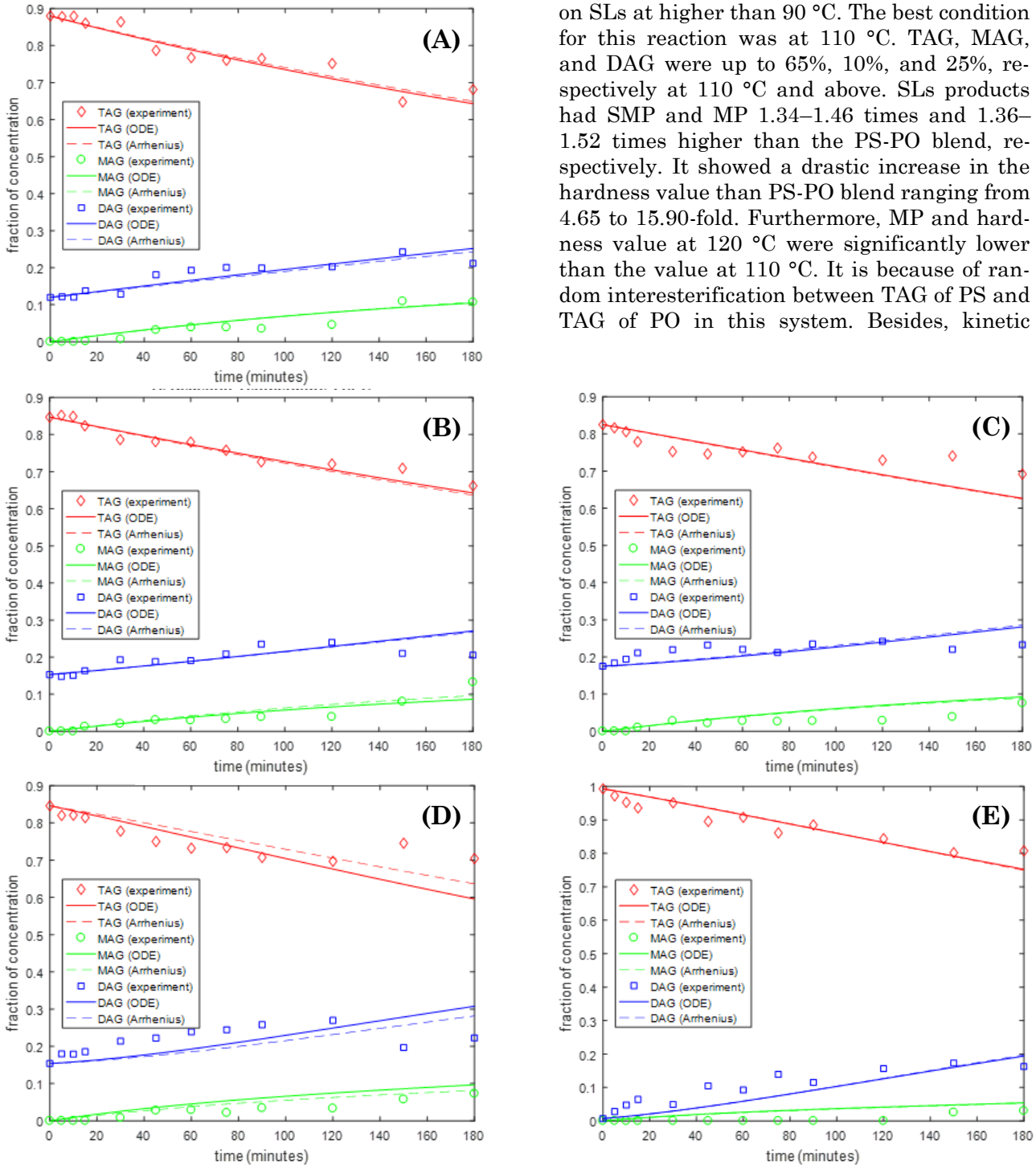

Figure 4. Reaction kinetic model of TAG, MAG, and DAG at reaction temperature 120 °C (A), 110 °C (B), 100 °C (C), 90 °C (D), and 80 °C (E). 'Experiment' represents the experimental data, 'ODE' represents the model from differential equations, and 'Arrhenius' represents the model using Arrhenius parameters substitution.

models implied that the reaction could be irreversible at a higher temperature. Equation (3) is the dominant reaction in glycerolysis-interesterification, which leads to a higher content of DAG than MAG in the end product. In summary, glycerolysis-interesterification of PS-PO blend for producing SLs using the activated sodium silicate as catalyst improved MP, SMP, and hardness of SLs due to an increase in MAG and DAG content at a higher temperature.

Acknowledgments

This research was funded by the Ministry of Research and Technology / National Research and Innovation Agency of Republic Indonesia (RISTEK-BRIN) Research Grant "*Program Menuju Doktor Sarjana Unggul* (PMDSU) Batch III". Contract Number: 2972/UN1.DITLIT/DIT-LIT/LT/2019.

References

[1] Kim, B.H., Akoh, C.C. (2015). Recent Research Trends on the Enzymatic Synthesis of Structured Lipids. *Journal of Food Science*, 80(8), 1713–1724. DOI: 10.1111/1750-3841.12953.

[2] Naik, M.K., Naik, S.N., Mohanty, S. (2014). Enzymatic Glycerolysis for Conversion of Sunflower Oil to Food Based Emulsifiers. *Catalysis Today*, 237, 145–149. DOI: 10.1016/j.cattod.2013.11.005.

[3] Zhong, N., Cheong, L.Z., Xu, X. (2014). Strategies to obtain high content of monoacylglycerols. *European Journal of Lipid Science and Technology*, 116, 97–107. DOI: 10.1002/EJLT.201300336.

[4] Feltes, M.M.C., de Oliveira, D., Block, J.M., Ninow, J.L. (2012). The Production, Benefits, and Applications of Monoacylglycerols and Diacylglycerols of Nutritional Interest. *Food and Bioprocess Technology*, 6, 17–35. DOI: 10.1007/s11947-012-0836-3.

[5] Subroto, E., Supriyanto, S., Utami, T., Hidayat, C. (2018). Enzymatic glycerolysis–interesterification of palm stearin–olein blend for synthesis structured lipid containing high mono- and diacylglycerol. *Food Science and Biotechnology*, 28(2), 511–517. DOI: 10.1007/s10068-018-0462-6.

[6] Subroto, E., Wisamputri, M.F., Supriyanto, S., Utami, T., Hidayat, C. (2020). Enzymatic and chemical synthesis of high mono- and diacylglycerol from palm stearin and olein blend at different type of reactor stirrers. *Journal of the Saudi Society of Agricultural Sciences*, 19(1), 31–36. DOI: 10.1016/j.jssas.2018.05.003.

[7] Reyniers, M.F., Marin, G.B. (2014). Experimental and Theoretical Methods in Kinetic Studies of Heterogeneously Catalyzed Reactions. *Annual Review of Chemical and Biomolecular Engineering*, 5, 563–594. DOI: 10.1146/annurev-chembioeng-060713-040032.

[8] Daramola, M.O., Nkazi, D., Mtshali, K. (2015). Synthesis and Evaluation of Catalytic Activity of Calcined Sodium Silicate for Transesterification of Waste Cooking Oil to Biodiesel. *International Journal of Renewable Energy Research*, 5(2), 517–523. DOI: 10.20508/ijrer.v5i2.2164.g6606

[9] Okullo, A.A., Temu, A.K. (2015). Modelling the Kinetics of Jatropha Oil Transesterification. *Energy and Power Engineering*, 7, 135–143. DOI: 10.4236/epe.2015.74013.

[10] Vallance, C. (2017). Rate laws: relating the reaction rate to reactant concentrations. In *An Introduction to Chemical Kinetics*. California: Morgan & Claypool Publishers.

[11] Darnoko, D., Cheryan, M. (2000). Kinetics of Palm Oil Transesterification in a Batch Reactor. *Journal of the American Oil Chemists' Society*, 77(12), 1263–1267. DOI: 10.1007/s11746-000-0198-y.

[12] Kumoro, A.C. (2012). Experimental and Modeling Studies of the Reaction Kinetics of Alkaline-Catalyzed Used Frying Oil Glycerolysis using Isopropyl Alcohol as a Reaction Solvent. *Research Journal of Applied Sciences, Engineering and Technology*, 4(8), 869–876.

[13] Solaesa, A.G., Sanz, M.T., Beltran, S., Melgosa, R. (2016). Kinetic study and kinetic parameters of lipase-catalyzed glycerolysis of sardine oil in a homogeneous medium. *Chinese Journal of Catalysis*, 37, 596–606. DOI: 10.1016/S1872-2067(15)61040-3.

[14] Voll, F., Kruger, R.L., Castilhos, F., Filho, L.C., Cabral, V., Ninow, J., Corazza, M.L. (2011). Kinetic modeling of lipase-catalyzed glycerolysis of olive oil. *Biochemical Engineering Journal*, 56, 107–115. DOI: 10.1016/j.bej.2010.11.005.

[15] Moquin, P.H.L., Temelli, F., King, J.W., Palcic, M.M. (2005). Kinetic Modeling of the Glycerolysis Reaction for Soybean Oils in Supercritical Carbon Dioxide Media. *Journal of the American Oil Chemists' Society*, 82(2), 613–617. DOI: 10.1007/s11746-005-1118-x.

[16] Zhong, N., Deng, X., Huang, J., Xu, L., Hu, K., Gao, Y. (2014). Low-temperature chemical glycerolysis to produce diacylglycerols by heterogeneous base catalyst. *European Journal of Lipid Science and Technology*, 116(4), 470–476. DOI: 10.1002/ejlt.201300438.

[17] Corma, A., Iborra, S., Miquel, S., Primo, J. (1998). Catalysts for the Production of Fine Chemicals: Production of Food Emulsifiers, Monoglycerides, by Glycerolysis of Fats with Solid Base Catalysts. *Journal of Catalyst*, 173, 315–321. DOI: 10.1006/JCAT.1997.1930.

[18] Zhang, Z., Ma, X., Wang, Y., Yan, R., Liu, M. (2014). Production of Monoacylglycerols from Fully Hydrogenated Palm Oil Catalyzed by Hydrotalcite Loaded with K2CO3. *Chemical Engineering Communications*, 202(5), 585–592. DOI: 10.1080/00986445.2013.853294.

[19] Guo, F., Peng, Z.G., Dai, J.Y., Xiu, Z.L. (2010). Calcined sodium silicate as solid base catalyst for biodiesel production. *Fuel Processing Technology*, 91, 322–328. DOI: 10.1016/j.fuproc.2009.11.003.

[20] Perdana, I., Nugrahanti, N., Sofiyah, S., Bendiyasa, I.M. (2016). Transesterification of palm oil using sodium silicate base catalyst from geothermal sludge. *IOP Conference Series: Materials Science and Engineering*, 162, 012–024. DOI: 10.1088/1757-899X/162/1/012024

[21] Tanabe, K., Yamaguchi, T. (1963). Basicity and Acidity of Solid Surfaces. *Journal of the Research Institute for Catalysis Hokkaido University*, 11(3), 179–184.

[22] Anggoro, D.D., Buchori, L., Sumantri, I., Oktavianty, H. (2019). Preparation and characterization of KF/CaO-MgO catalyst for monoglycerides synthesis. *Malaysian Journal of Fundamental and Applied Sciences*, 15(5), 640–643. DOI: 10.11113/mjfas.v15n5.1243.

[23] AOCS. (1997). Official and Tentative Methods of the American Oil Chemist's Society, 7th Ed. Champaign, Illinois: American Oil Chemist's Society Press USA.

[24] Coates, J. (2006). Interpretation of Infrared Spectra, A Practical Approach. In *Encyclopedia of Analytical Chemistry*. Chichester: John Wiley & Sons, Ltd. DOI: 10.1002/9780470027318.a5606.

[25] Guo, F., Wei, N.N., Xiu, Z.L., Fang, Z. (2012). Transesterification mechanism of soybean oil to biodiesel catalyzed by calcined sodium silicate. *Fuel*, 93, 468–472. DOI: 10.1016/j.fuel.2011.08.064.

[26] Xie, W., Peng, H., Chen, L. (2006). Calcined Mg–Al hydrotalcites as solid base catalysts for methanolysis of soybean oil. *Journal of Molecular Catalysis A: Chemical*, 246, 24–32. DOI: 10.1016/j.molcata.2005.10.008.

[27] Dijkstra, A.J. (2020). Some Thoughts on the Mechanism of Ester Interchange Reactions Involving Acylglycerols. *European Journal of Lipid Science and Technology*, 122, 1–7. DOI: 10.1002/ejlt.202000188.

[28] Zhong, N., Li, L., Xu, X., Cheong, L.Z., Xu, Z., Li, B. (2013). High yield of monoacylglycerols production through low-temperature chemical and enzymatic glycerolysis. *European Journal of Lipid Science and Technology*, 115(6), 684–690. DOI: 10.1002/ejlt.201200377.

[29] Aini, I.N., Miskandar, M.S. (2007). Utilization of palm oil and palm products in shortenings and margarines. *European Journal of Lipid Science and Technology*, 109, 422–432. DOI: 10.1002/ejlt.200600232.

[30] Kellens, M., Gibon, V., Hendrix, M., Greyt, W.D. (2007). Palm oil fractionation. *European Journal of Lipid Science and Technology*, 109, 336–349. DOI: 10.1002/ejlt.200600309.

[31] Soares, F.A.S.D.M., da Silva, R.C., da Silva, K.C.G., Lourenco, M.B., Soares, D.F., Gioielli, L.A. (2009). Effects of chemical interesterification on physicochemical properties of blends of palm stearin and palm olein. *Food Research International*, 42, 1287–1294. DOI: 10.1016/j.foodres.2009.03.022.

[32] Gulyaev, I.P., Soloneko, O.P. (2013). Hollow droplets impacting onto a solid surface. *Experiments in Fluids*, 54(1432), 1–12. DOI: 10.1007/s00348-012-1432-z.

[33] Jia, D., Hamilton, J., Zaman, L.M., Goonewardene, A. (2007). The time, size, viscosity, and temperature dependence of the Brownian motion of polystyrene microspheres. *American Journal of Physics*, 75(2), 111–115. DOI: 10.1119/1.2386163.

[34] Dijon, A. (2015). Microwave-irradiated zinc chloride catalyzed glycerolysis of high free fatty acid vegetable oil. *Master Thesis*, Gokongwei College of Engineering, De La Salle University.

[35] Gole, V.L., Gogate, P.R. (2014). Intensification of glycerolysis reaction of higher free fatty acid containing sustainable feedstock using microwave irradiation. *Fuel Processing Technology*, 118, 110–116. DOI: 10.1016/j.fuproc.2013.08.018.

[36] Satriana, S., Supardan, M.D. (2008). Kinetic Study of Esterification of Free Fatty Acid in Low Grade Crude Palm Oil using Sulfuric Acid. *ASEAN Journal of Chemical Engineering*, 8(1), 1–8. DOI: 10.22146/ajche.50112.

[37] Susanti, R.F., Kim, J., Yoo, K. (2014). Supercritical Water Gasification for Hydrogen Production. In *Supercritical Fluid Technology for Energy and Environmental Applications*. Oxford: Elsevier B.V. DOI: 10.1016/B978-0-444-62696-7.00006-X.

[38] Moquin, P.H.L., Temelli, F., King, J.W., Palcic, M.M. (2005). Kinetic Modeling of the Glycerolysis Reaction for Soybean Oils in Supercritical Carbon Dioxide Media. *Journal of the American Oil Chemists' Society*, 82(2), 613–617. DOI: 10.1007/s11746-005-1118-x.

[39] Mozurkewich, M., Benson, S.W. (1984). Negative Activation Energies and Curved Arrhenius Plots. 1. Theory of Reactions over Potential Wells. *The Journal of Physical Chemistry A*, 88, 6429–6435. DOI: 10.1021/j150669a073.

[40] Lionelli, S. (2019). What distinguishes data from models?. *European Journal for Philosophy of Science*, 9(22), 1–27. DOI: 10.1007/s13194-018-0246-0.